J. Ind. Geophys. Union (July 2007)
Vol.11,No. 3,pp.157-170

RF Emissions, Types Of Earthquake Precursors: Possibly Caused By The Planetary Alignments

V G Kolvankar

Seismology Division, Bhabha Atomic Research Centre, Trombay, Mumbai 400 085
Email: vkolvankar@yahoo.com

ABSTRACT

Various research workers have reported EM emission prior to earthquakes or during an earthquake sequence. In few cases, these EM emissions were consistently found during certain hours of the day. EM emission in semi-diurnal pattern spaced in time domain from the local noontime was observed in many examples prior to earthquakes / volcanic eruption. Also such emission was observed in a very wide frequency band from VLF to Microwave range. Besides this semi diurnal type of pattern, some other type of EM emission had diurnal pattern. This type was witnessed in Valsad [1991] and Chilean earthquake sequence [1960], in which it preceded semidiurnal pattern found in these earthquake sequences. The cause of this type of EM emission seems to be completely different than that for semidiurnal type. Efforts are made here to check whether the gravitational forces of the planetary alignments caused these types of RF emission. This paper discusses all these examples in details and discusses an application for the development of reliable monitoring of Earthquake/ Volcanic eruption precursors in the high seismicity area.

Keywords: Telemetered network, semi-diurnal, diurnal RF emission, earthquake sequence

Introduction

Many research workers have reported EM emissions prior to earthquakes and volcanic eruptions. Among these, semidiurnal types (twice in a day) are commonly seen. However diurnal type [once in a day] of EM emissions were also noticed in few cases.

Both these types of EM emissions were observed during the operation of an indigenously built radio telemetered seismic network (RTSN) which was commissioned at Bhatsa, (20º 37 N, 73º 18 E) Maharashtra state, India, to study the reservoir-induced seismicity (RIS) of the region and operated during 1989-1995[1]. RF interference to the radio links operated in UHF (Ultra High Frequency) band was witnessed prior to, during and after the earthquake sequence from Valsad region. Both these types of RF emissions are discussed in detailed.

Semidiurnal type of EM emissions related to earthquakes and volcanic eruptions were also observed in many other cases, which are briefly described in this paper.

One addition case of diurnal type of EM emission related to great Chilean earthquake was observed, which is also discussed here. Since the timings and nature of these types of EM emissions were found to be different, it is presumed that the causes for such disturbances are different than those for semidiurnal type. This paper also discusses the possible causes for these two types of EM emissions.

Finally based on the nature of these kinds of EM emissions a system for reliable monitoring of Earthquake/ Volcanic eruption precursor in the high seismicity areas is also suggested.

Few cases of Semidiurnal type of EM emissions related to earthquakes and volcanic eruptions: Many research workers witnessed similar semidiurnal type EM emission related to earthquakes and volcanoes in different frequency band starting from very low frequency (VLF) to microwave range. These were found twice during the day at timings equally spaced from local noontime. Followings are few such examples.

1. The recording of diurnal signal intensity envelope at frequency of 10 MHz on the Washington-Huankayo path prior to the disastrous quake in Chile (22nd May 1960), had a pronounced 24-hour variation in the shape of a wave minimum at 14-21 hours UT (day interval) and maximum 23-11 hours (night interval), mainly caused by ionosphere changes and signal gradually rising over 20-00 hours and decreasing over 11-14 hours[2]. Anomalies in terms of sharp variations were noticed between 08-12 hours and 19-00 hours almost all these days (17-23 May 1960), which had linearly modulated this intensity envelope. The onset timings of the major foreshock,

main shock and aftershocks also correspond to the timing of these anomalies.

2. Yamamoto Isao et.al. (2002) generated a system for earthquake prediction research in the region of VHF frequency band. EM noise of the atmospherics at the ORSOC (Okayama Ridai Seismic Observatory Center, E 144-55'48. 3", N34-41'48. 1") and its neighborhood was carried out using multiple antennas in VHF band. EM noise was experienced at 09-11 hours and 12:30-14:30 local time and the same noise affected the whole FM band[3]. Four events (Source: NEIC-USGS), which fell within ± 500 km range, occurred within three days of this type of RF emission (on 17.07.2001) close to ORSOC. Two of these four events seem to have occurred during the timings of second of the semi-diurnal RF emission.

EQ /VOLCANO SEQUENCE - FREQ-BAND OF EM EMISSION	PERIOD OF SEMI-DIRUNAL EM EMISSION	TIMING OF THE FIRST EM EMISSION	TIMING OF THE SECOND EM EMISSION	LOCAL NOON TIME & TIME OFFSET OF EM EMISSIONS	OCCURRENCE OF EARTHQUAKE-VOLCANIC ERUPTION	REMARKS
Valsad, India. UHF RANGE 460-461 MHz.	10 –30 April 1991	0400 GMT (0900 LT) Duration 10-100 min. approx.	1200 GMT (1700 LT) Duration 10-100 min. approx	0800 GMT (1300 IST) Approx. RF emission timings are offset by ± 4 hours	04:17(GMT) on 14.04.1991 foreshock 05:13 hrs (GMT) on 30-04-1991 Main shock	The timings of the main shock and one of the two foreshocks closely match the timing of the first RF emission. Semidiurnal type EM emission seized after the main shock
Chilean Earthquake HF 10 MHz and HF 18 MHz (J W. Warwick et. al.)	16-23 May 1960	08-12 Hrs GMT	19-24 Hrs GMT	1700 GMT approx. RF emission timings are offset with noontime by ± 5 hours	All six earthquakes, with magnitude range of 6.7 –9.5 occurred within the timings of RF emission.	These six events consist of two foreshocks, main shock and three aftershocks listed in the book "Earthquake prediction Seismo-electromagnetic phenomena"
ORSOC (Okayama Ridai Seismic Observatory Center) VHF - 76-108 MHz	17.07.2001 (as indicated in the diagram of the paper)	09-11 Hrs JST	12-30 – 14-30 JST	1200 hrs approx. emission timings are offset with noontime by ±1.5 hours	Four events occurred within the time period of 3 days of the RF emission occurrence. (Source NEIC USGS) The timings of two of them match with the timings of the second RF emission.	The details are taken from the paper[5]. RF Emission received on an array of VHF receivers on 17.07.2001. However the authors have not provided any correlation of this RF emission with any seismic activity. Four events occur within three days of this emission, which lie within ± 4 deg Long and ± 5 deg of Lat from ORSOC.
Precursory Signature effect of the Kobe earthquake of VLF sub-ionospheric signals. VLF range 10.2 KHz and 11.3 KHz	Jan 03-23,1995 and continued beyond this period	0830 hours JST	1630 Hours JST	Around 12-30 Hours JST Timings of the VLF phase reaching minimum are offset with noontime by ± 4.0 hours	Sudden changes in the phases prior to main shock on 17th Jan 1995 The timings of these VLF signal phase reaching minimum are spaced equally from the noon local time. Kobe earthquake timings (0546 Hrs) differ by couple of hours to the first VLF phase min. timing.	The sub-ionospheric VLF Omega signal transmitted from Tsushima (34°37'N, 129°27' E), Japan, is continuously received at Inubu (35°42'N,140°52'E). The signal propagation characteristics (phase in particular) exhibited abnormal behavior (especially around the sunrise and sunset local times) a few days before the main shock of 1995.
Apollo Lunar Seismic data for stations 12 and 16 Microwave range 1-2 GHz	Seen continuously through out the Lunar seismic data for period (1969-1977)	Around 10 days (Solar) from new Moon Lunar days for station 12 Around 07 days (Solar) from new Moon Lunar days for station 16	Around 23 days (Solar) from new Moon Lunar days for station 12 Around 20 days (Solar) from new Moon Lunar days for station 16	Around 16.5 days (Solar) from new Moon Lunar days for station 12 Around 13.5 days (Solar) from new Moon lunar days for station 16	Details of events close to Stn. 12 & 16 are not known However A1 (One of the major location of seismically active region at deeper level) events were observed only during 15-20, and 7-12 Lunar days (sidereal phase) from new moon day. This variation caused due to nodding of moon from $+5^0$ --5^0 (1970-1978)	Apollo Lunar Seismic data of stations 12 and 16 provided noisy signals near the times of Lunar sunrise and sunset, even accompanied with spikes. The three days (Solar day) offset in time of sunrise/sunset for station 12 and 16 reflects 39 degrees difference in longitude between the stations. The local noisy period, around 10 & 23 days for station 12 around 7 & 20 days (from new moon) for station 16, is not simultaneous and vary with longitude.
Mt Mihara Volcano, Japan Ohshima Island, LF - 82 KHz	03-21 Nov 1986	09-11 Hrs JST	14-16 Hrs JST	1230 Hrs JST – RF emission timings are offset with noontime by ±2.5 hours	Ist eruption at 1725 Hrs JST, Nov 15, 1986 2nd eruption 1615 Hrs JST, Nov 21, 1986	Both eruptions occurred within the timings of the EM emissions

Table 1. Details of all the six examples of semi-diurnal EM emission spaced equally from the local noon timings.

3. Haykawa M, Molchanov O A, Tondoh T and Kawai E studied precursory signature effect of the Kobe earthquake of VLF sub-ionospheric signals transmitted from Tsushima (34°37'N, 129°27'E), Japan, was continuously received in Inubu (35°42'N, 140°-52'E). The signal propagation characteristics (phase in particular) exhibited abnormal behavior (especially around the sunrise and sunset local times) a few days before the main shock of the 17th Jan 1995. The timings of these VLF signals phase reaching minimum, again spaced equally from the noon local time. The Kobe earthquake (0546 Hrs.) occurred couple of hours prior to the first VLF phase minimum timing[4].

4. Apollo Lunar Seismic Experiment (APSE) consisted of four seismic stations commissioned on lunar surface between 1969 and 1972. Each station included a tri-axial long period and a vertical short period instrument. The data was telemetered to earth and recorded until 1977. Deep moon quakes at the depth 700-1000 km dominate the entire collection of data and show good correlation with the tidal stresses[5].

It is seen from the record that the noisiest part of the record occur near the timings of lunar sunrise and sunset, even accompanied with spikes. The three days (solar day) offset in time of sunrise/sunset for station 12 and 16 (commissioned during Apollo 12 and Apollo 16 missions respectively) reflects difference of 39 degrees in longitudes of two stations. This indicates that the local noisy period is not simultaneous and varies with longitude. The pattern is similar to semi-diurnal pattern seen on the earth at different longitudes.

5. Takeo Yoshino and Ichro Tomizawa (1989) observed low frequency (82 KHz) EM emission at precursors to the volcanic eruption at Mt. Mihara during Nov.1986. Several clear bursts like emission were gathered during Nov. 3 to 22. The EM emissions were confined to 09 to 11 and 14 to 16 hours (JST) only[6]. Besides the timings of the first eruption in creator A (at 17:25 hours on Nov 15,1986) and simultaneous eruption in multiple creator C (at 16:21 hours on 21st Nov 1986) match with the timings of the EM emission observed.

Table 1 provides the details of semi-diurnal EM emissions in all above cases including the RF disturbance presumably related with Valsad earthquake sequence.

RF disturbance related to Valsad earthquake sequence: The RTSN at Bhatsa had 9 field stations spread over an area of around 500 sq. km. Each station had a single vertical seismometer and frequency modulated analog signals were telemetered to the base station via individual links operated at the spot frequency in UHF band (461- 462 MHz), on a 24 hours basis. The data from this network was edited online and the event portion with about 15 sec. of pre-event portion was recorded on a magnetic tape, in digital format[1]. The layout of the Bhatsa network is provided in Fig. 1.

This network recorded an earthquake sequence from Valsad region located at a distance of 115 km north of this network. Nearly 400 events in the Magnitude range of 1.4 to 5.0 were recorded from 25th March 1991 to 30th June 1991 with the main event of Magnitude 5.0 on 30th April (05:13:56 GMT) 1991.

Three weeks prior to the start of the earthquake sequence, intense diurnal type of disturbances, were witnessed during 5th –11th March 1991 only at certain timings (close to 00:00 hours GMT) and the entire network was disrupted for few minutes on five different occasions. After the start of the earthquake sequence (on 25th March 1991), RF disturbances of semidiurnal type were observed only during certain timings (04 and 12 Hours GMT) of the day.

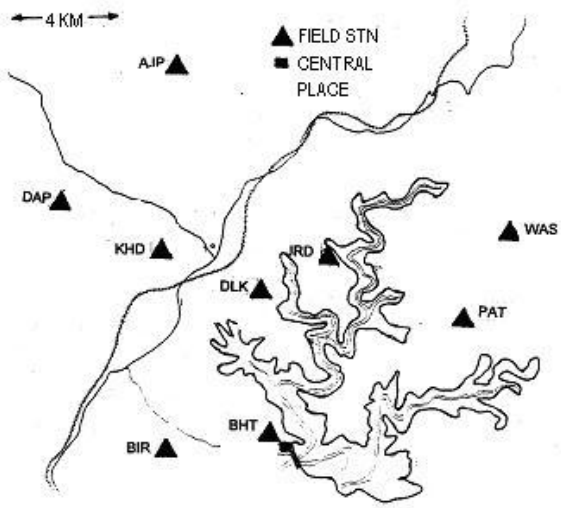

Fig. 1. Layout of the RTSN at Bhatsa, India.

Fig. 2 provides overall picture of the RF disturbance for period of 1st March (day 60) till the end of August 1991. Caption under this figure provides the details of the overall RF disturbance experienced by this network.

A specimen of the diurnal type RF disturbance is provided in the Fig. 3. In this figure only the starting portion of the RF disturbance (at 23:57:00 on 8th March 1991) as well as the end portion (at 00:18:00 on 9th March 1991) are illustrated in separate parts. As illustrated in this figure the end portion of the RF disturbance provides an exact mirror replica of the starting portion.

Table 2 provides the details of the RF disturbance during pre-earthquake sequence period. It is evident from this table that consecutively for eight days (barring day 65) the RF disturbance was experienced close to 00 hours (GMT) in most of the RF links of the network.

After the V G Kolvankar onset of the earthquake sequence, the RF disturbances observed were of much longer duration extending to over 100 minutes and were confined to the disturbances of telemetry links from stations situated in the northern region only. Only the receivers with antennas pointing towards north were affected by these disturbances. However in cases of RF disturbances prior to the occurrence of the Valsad earthquake sequence, it was observed that most RF links were affected, which include stations in east and west directions indicating that they must be much stronger than the RF disturbances experienced when the earthquake sequence was on.

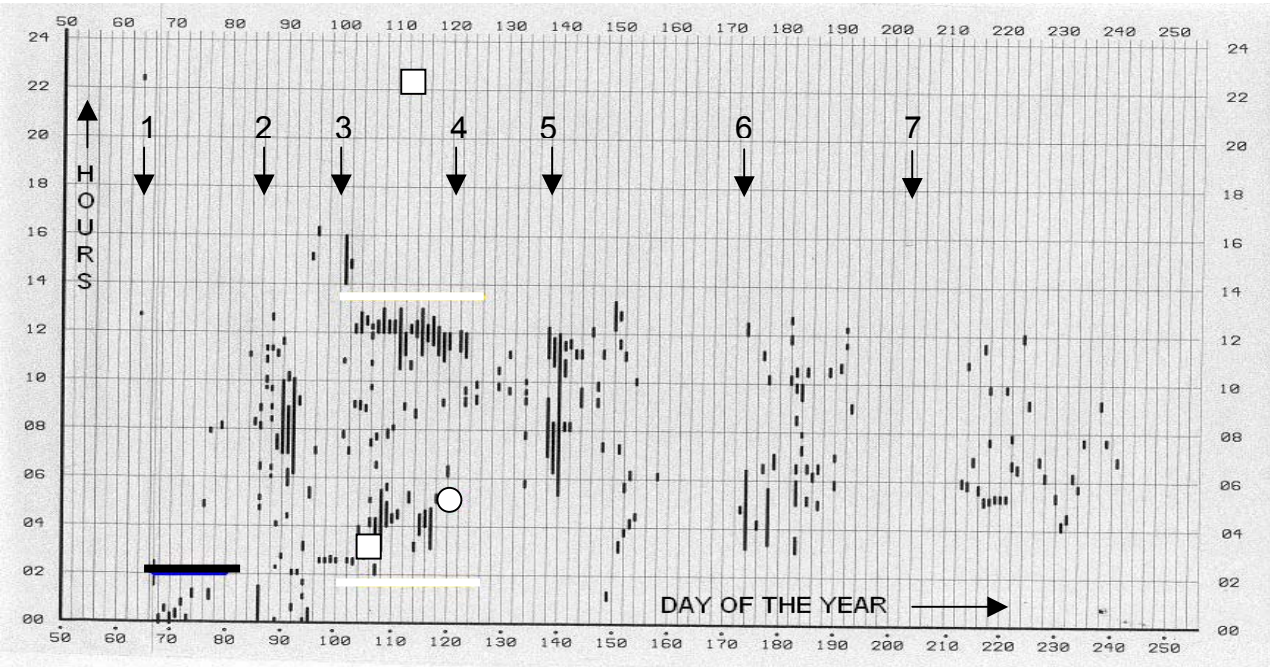

Fig. 2: Picture of the RF disturbance for period of 1st March (day 60) till the end of August 1991. In this figure each vertical line represents a day and it is segmented every 2 hours. For convenience lines are shown for alternate days. Thick lines indicate the RF activities and their lengths indicate the duration. For the sake of noticeable display, longer lines are drawn for short duration disturbances (in the order of few seconds]. Positions of two foreshocks are shown with small squares and that of the main event with a small circle. The timings of the main event and one of the foreshock match with timings of the EM emission at around 0400 hours. ***[Semi-diurnal portion of the RF disturbance is indicated within a pair of broad white color lines (between arrows 3&4), where as the diurnal portion is indicated under thick black color line]***
The indications of arrows are as follows:
Arrow 1: Start of the RF disturbance in the radio links at around 00 hours GMT.
Arrow 2: Start of the earthquake sequence.
Arrow3: Occurrence of major foreshock, RF disturbance shifted to around 04 and 12 hours GMT
Arrow 4: Occurrence of major Shock of Mg. 5.0 RF disturbance pattern changes.
Arrow 5 and 6: RF disturbances associated with few aftershocks of Mg. 2.5-3.5.
Arrow 7: End of earthquake sequence. However RF disturbance continued in patches for 2 months.

Generation of the RF emission envelope: Fig. 3 provides starting portion and end portion of the RF disturbances of equal length. If all these starting and end portions of different links in the Bhatsanet are rearranged in terms of the received signal strength then they would provide an envelop of rising and falling RF emission signals as illustrated in Fig. 4. The RF links provide noisy signals when the RF emission signals overcome the signals received from the field stations. In reality the RF emission envelope steadily raises from low level to high level within a minute interval, stays at this level for interval of few minutes accompanied with few variations and then steadily falls from high level to low level.

In order to study the causes of these phenomena, the following experimental facts, observed in relation to UHF telemetry of the seismic analog signals, may be noted.

The received signal strength of the telemetry links depend on various factors such as transmitted power, receiver sensitivity, antennas gains, distance between the field station and the central place, type of terrain etc. With all these factors, the received signal strength for different links at any time could lie within 10 – 30 dB above the noise level.

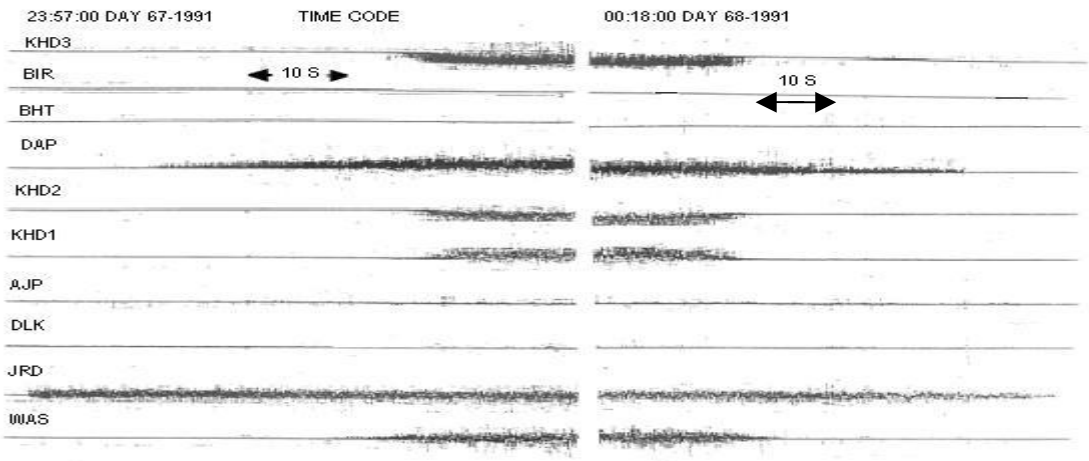

A B

Fig. 3. The starting portion (23:57:00 on day 67, 8th march 1991) and end portion of the RF disturbance 00:18:00 on day 68, 9th March 1991 are illustrated on a multi-channel seismic noise sample at low sensitivity, which normally should provide straight lines. The latter portion provides exact mirror replica of the starting portion of this RF disturbance. KHD station had tri-axial sensor and three component analog data was telemetered using FDM (frequency division multiplexing) technique.

SER. NO.	DATE[DAY]	TIME	DURATION	REMARKS
1	05.03.91[64]	01:25:20	300 Sec.	Seen in AJP and PAT helical records
2	05.03.91[64]	12:45:30	40 Sec.	**All working channels affected**
3	05.03.91[64]	22:17:06	270 Sec.	Seen in AJP and PAT helical records
4	08.03.91[67]	01.28.10	180 Sec.	**All working channels affected**
5	08.03.91[67]	23:57:00	7.5 – 23 Min.	**All working channels affected**
6	09.03.91[68]	23:56:30	22 Min.	**All working channels affected**
7	10.03.91[69]	00:37:00	120 Sec.	Multi-channel play-out available
8	10.03.91[69]	23:53:20	100 Sec.	Seen in AJP helical records
9	11.03.91[70]	23:56:00	13 Min.	**All working channels affected**

Table 2: Details of the RF disturbance experience by Bhatsa network prior to the onset of the earth quake sequence on 25th March 1991. AJP, PAT, JRD, DAP are the short forms of few field stations. The signals from AJP and PAT stations were monitored on helical drum recorder on 24-hour basis.

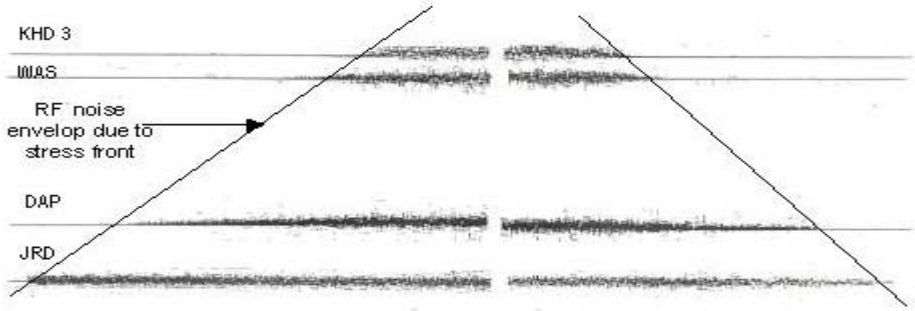

Fig. 4. Starting and end portions of different links in the Bhatsa net are rearranged in terms of the received signal strength then they would provide an envelop of rising and falling RF emission signals. The other channel links (BIR, BHT, AJP, DLK) have also provided noise of much shorter duration and hence

those corresponding noise portions do not figure in this diagram. The KHD stations had a tri- axial seismic sensor and hence the duration of noise portions were identical for all three signals from this station.

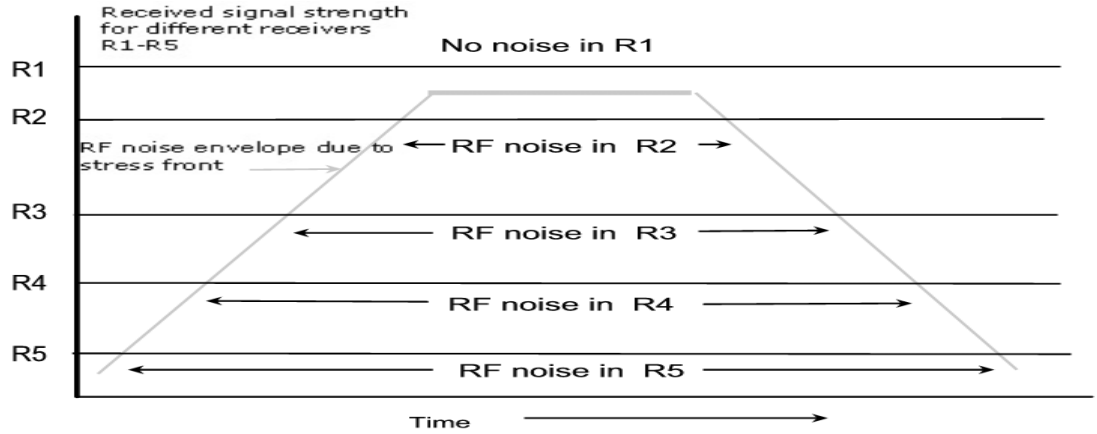

Fig. 5. General noise envelope and length of RF noise, which could be seen in different receivers out put with different receiver strength indicated by R1- R5. The received signal strength in R1 is above the level of RF noise generated by the stress pulse and hence shall not provide any noise. The rise and fall time of this stress pulse was about a minute interval in Bhatsanet.

In Fig. 5, it is demonstrated that if the strength of the stress front gradually increases and the RF noise generated by this stress front (which is experienced as broadband noise by different workers) also goes up proportionally, then the signals of the telemetry links cuts off when the RF noise exceeds the received signal strength. Since the received signal strength for different radio links within the RTSN are different as discussed earlier, the different links cut off at different time. Again, when the stress front recedes, the RF noise generated by it goes down proportionately and goes below the different received signal strengths at different time intervals. Fig 5, illustrates how this results in equal start and stop RF noise for each RF link, thereby generating mirror images of start and stop RF disturbances as illustrated in Fig. 3.

Few additional details of the diurnal type RF emission observed at Bhatsa net: Diurnal type RF emissions were observed during the week of 5th-11th March 1991 (about three weeks before the start of earthquake sequence on 25th March 1991). As said earlier the data for edited seismic events was obtained in online mode.

The event detection was carried out by comparing short term average (STA) and long term average (LTA) in multiple channel and was very reliably done for all earthquake data which generally have impulsive onsets[1]. However the RF disturbance data, which had slow rise and fall, was not triggered and recorded 100 %. However few of these RF disturbances were triggered online and recorded on the magnetic tape are being presented.

Fig 3A, 3B, 6, 7A, 7B, 11A and 12A provide multi-channel plot of the RF disturbances for dates 5th –11th March 1991 for the timings as per provided in table 1. Out of these Fig. 3A, 6, 7A, 7B, and 11A provide starting portions of RF disturbance and Fig. 2B, 12A provide end portion of the RF disturbances. Fig. 9 and 13 provide relevant portions of the helical record of continuous uninterrupted data of two radio-telemetered signals from AJP and PAT. The details of the records are provided in the caption under these figures.

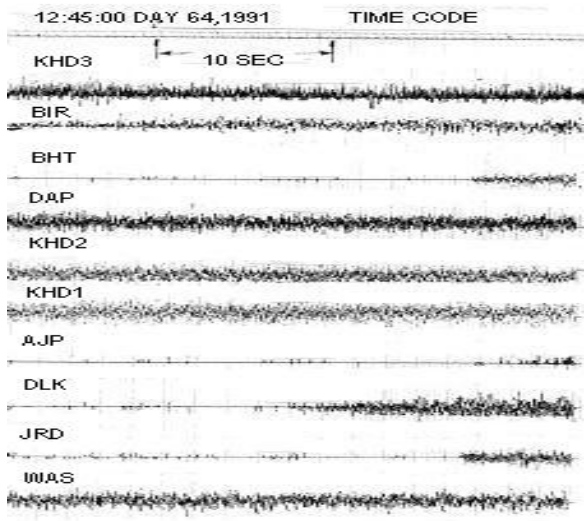

Fig. 6. A multi-channel plot of RF disturbance noticed on day [64] at 12.45.20 GMT. Three channels namely KHD, DAP and WAS were providing hash prior to the start of this record. BIR progressively started producing hash. Where as channels DLK, BHT, JRD and AJP started producing hash one after another in an interval of 20s.

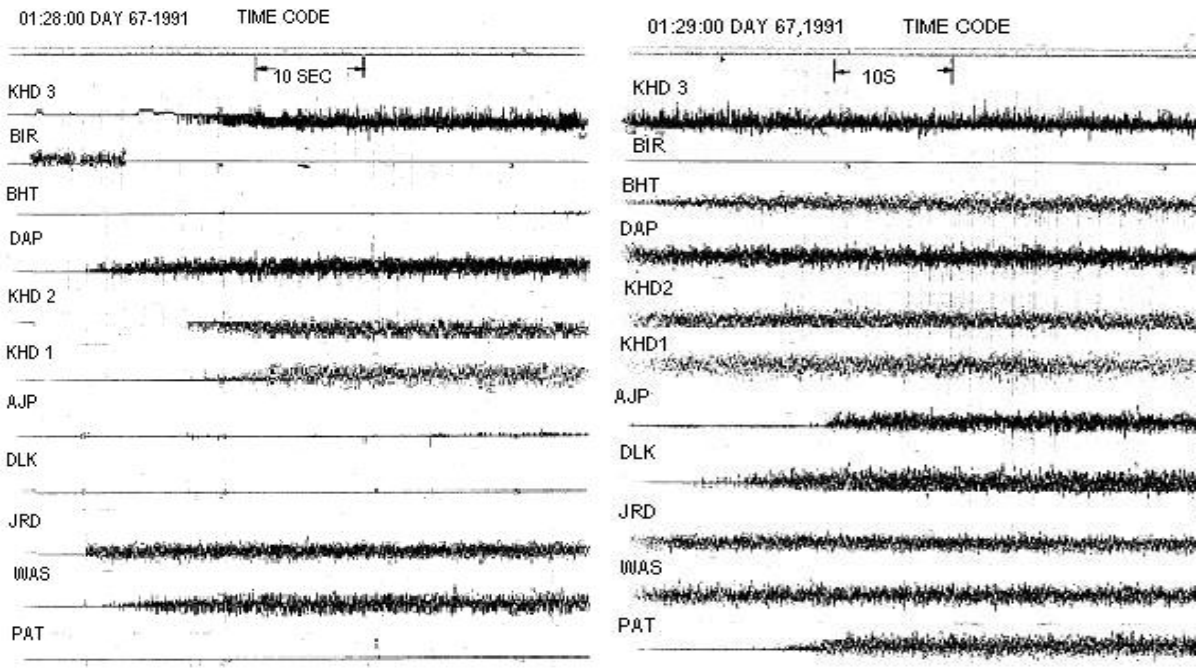

A B

Fig. 7. Part A illustrates a multi-channel play out of the hash signal. The record starts at 01:28:10 hours on 8th March 1991 (day 67). Channel JRD was providing hash at the start of the record. Channels DAP and WAS started producing hash just when the record started. Channel KHD started giving hash after about 10 seconds. Part B illustrates a portion of the record, which is continuous from record 7A. It indicate that channel BHT started producing hash at around 01:28:40 hours and stations at AJP and PAT started producing hash 20 seconds later. Both Fig. 7 A and B are very important due to the fact that it provides relative timings of the onsets of RF disturbances in all working channels.

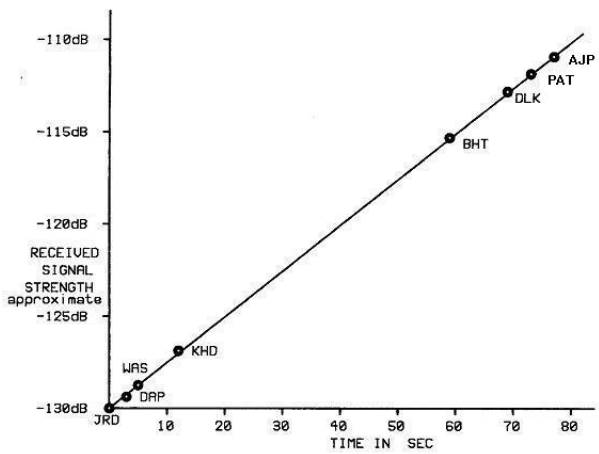

Fig. 8 provides the graph for the onset timings of RF disturbances Vs approximate strength of received signal from field stations. The relative timings for all network stations on horizontal scale are with respect to the JRD station in which the RF disturbance was first initiated. The vertical scale indicates approximately the strength of the received signal from all these stations.

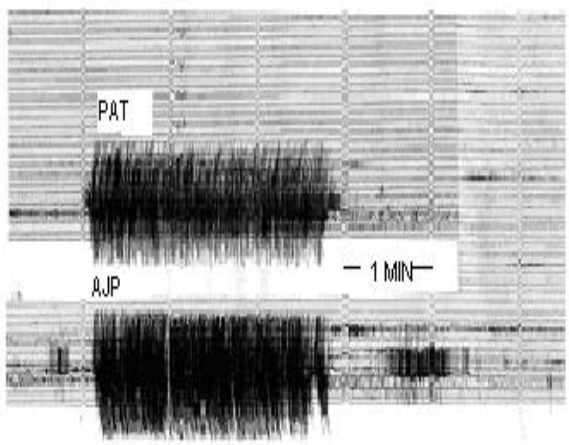

Fig. 9 Indicates PAT and AJP channel monitored on helicorder, had produced continuous hash for nearly 160 seconds. AJP channel was also producing spiky signals before and after this patch of continuous hash, (01:28:10 DAY 67, 1991). Also the main portion of the PAT channel is larger (at both ends) than the AJP channel.

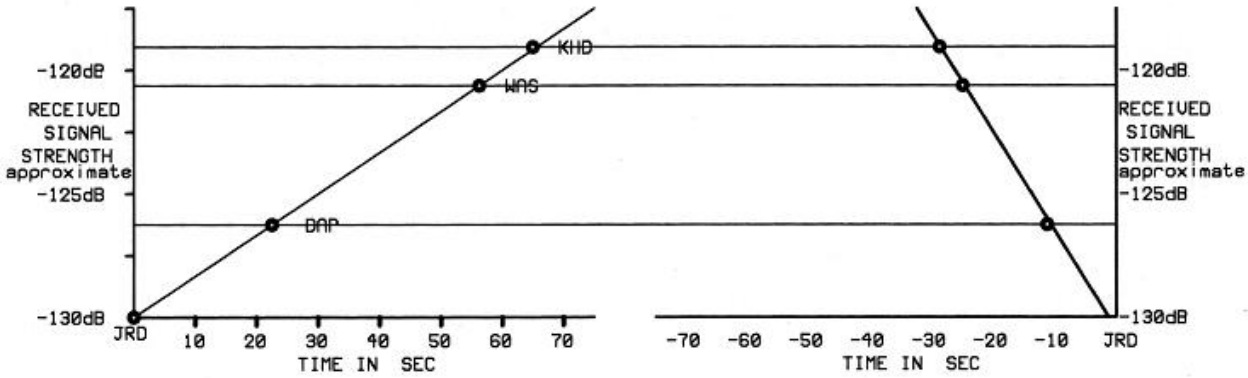

A **B**

Fig. 10. Provides the graph for the starting (part A) and end (part B) portion of RF disturbance record (displayed in Fig. 2) starting at 23:56:00 8th March (Day 67). The relative timings for all network stations on horizontal scale are with respect to the JRD station in which the RF disturbance was first initiated. These graphs resemble slopes of Fig. 8. However the slopes of these portions in time scale are different.

Fig. 8, 10A & B 11B & 12B provide graphs of relevant timings of the starting or end portion of the RF disturbances for all network stations on horizontal scale with respect to the JRD station (in which the RF disturbance was first initiated) Vs the approximately strength of the received signals from all these stations in vertical scale.

The sensitivity of all these receivers were 0.3 μV @ 12 dB SINAD equivalent to –146 dB. JRD station signal strength was assumed to be about 16 dB above this level. The relative signal strength is computed for all other stations considering linear increase in RF noise in time scale and also max signal in the order of –110dB [-80 dBm] level which was found in few receivers during the operation of this network. Station BIR did not function after the first record on March 11 at 12: 00 GMT.

From all these records following points were noted.

A. Starting and end of the RF disturbances are not simultaneous in all the RF links from remote field stations. Hence these types of disturbances due to power line fluctuations etc. are ruled out.

B. The starting sequence of RF disturbance in stations was found to be in the following order.

1- JRD, 2 - DAP, 3 - WAS, 4 - KHD, 5 - BHT, 6 – DLK, 7 – AJP, 8 – PAT. (Except in some cases AJP, PAT, which was very close in receiving signal strength, exchanged their positions).

RF disturbance shown in Fig. 6 for day (64) at 12.45.20 GMT indicate different order for four stations. However, the timings of this disturbance is totally different than those in other cases, which consistently showed timings around 00 hours GMT.

C. The end sequence of RF disturbance in stations was found to be exactly in reverse order. 1 - PAT, 2 - AJP, 3 - DLK, 4 - BHT, 5 - KHD, 6 – WAS, 7 – DAP, 8 – JRD.

D. Four of these eight stations were found to be at lower level of received field strength (-130dB to -126dB) whereas four other were at much higher received field strength (-115dB to – 110dB). This means that when the total network was inoperative the RF signal level was above –110dB.

The RF disturbance related to Valsad earthquake sequence is discussed in detail elsewhere[7].

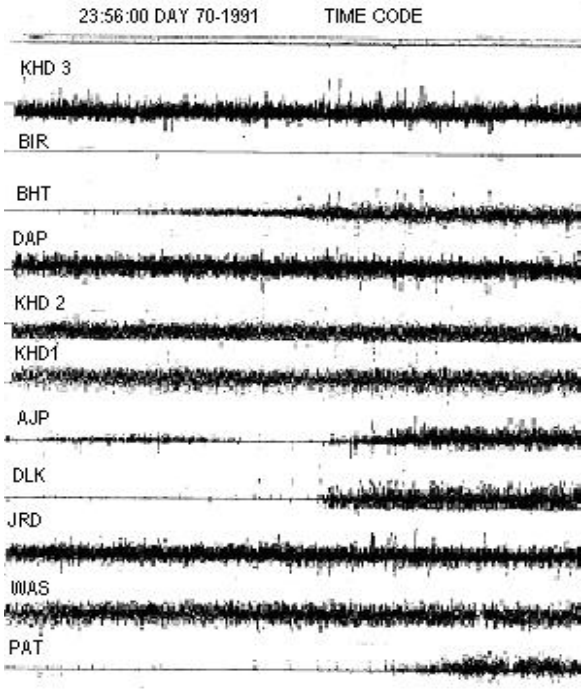

Fig 11A: A multi-channel record at 23:56:00 on 11th March [Day 70] is illustrated. Channels KHD, DAP, WAS, JRD were producing hash from the beginning of the record where as BHT, AJP, DLK and PAT stopped functioning within 30 seconds.

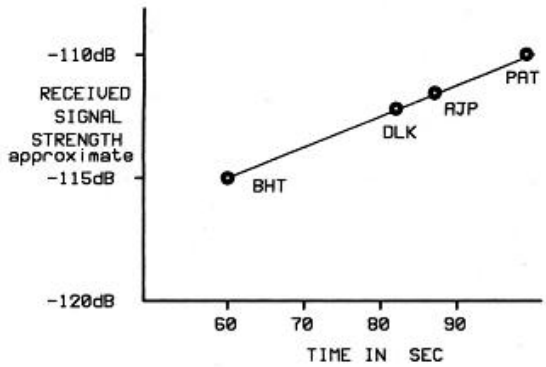

Fig 11B provide graph of the onset timings of RF disturbances Vs received signal strengths. The relative timings for all network stations on horizontal scale are with respect to the JRD station in which the RF disturbance was first initiated.

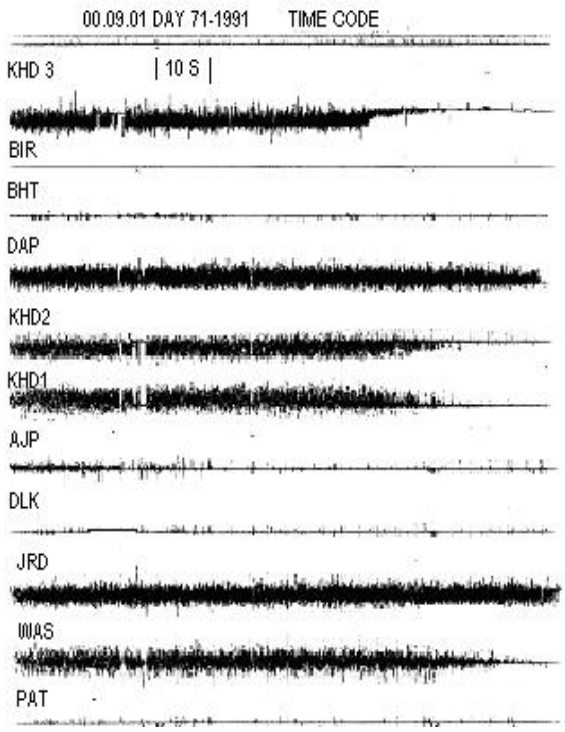

Fig 12A: A multi-channel record of 12th March at 00:09:00 hours. KHD, DAP and WAS stopped producing hash within about 30 seconds period.

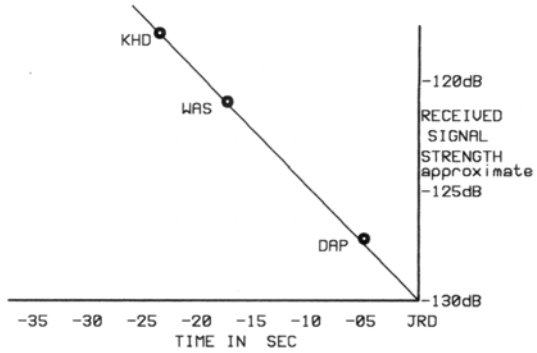

Fig 12B provide graph of the onset timings of RF disturbances Vs received signal strengths.

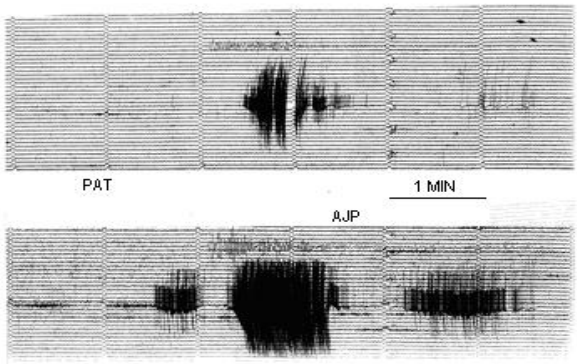

Fig 13: Helical records of PAT and AJP corresponding to multi-channel record of 11A (23:57:05 on 11th March). It seems from these records that the overall period of the hash was about 200 seconds.

Monitoring the local stress fronts: A grid of UHF/VHF links can be used to monitor the strength of various stress fronts in the seismically active region, which can provide warning of the impending earthquakes. A typical arrangement is illustrated in Fig. 14. As illustrated in this figure, a set of four receivers at the location of every big black dot shall receive signals from four transmitters located at four corners (indicated by small black dots) of a square of size 50 km X 50 km and operated at different spot frequencies in UHF/VHF band. The transmission can be through omni directional antenna since receivers in the adjacent block can also monitor the same signal.

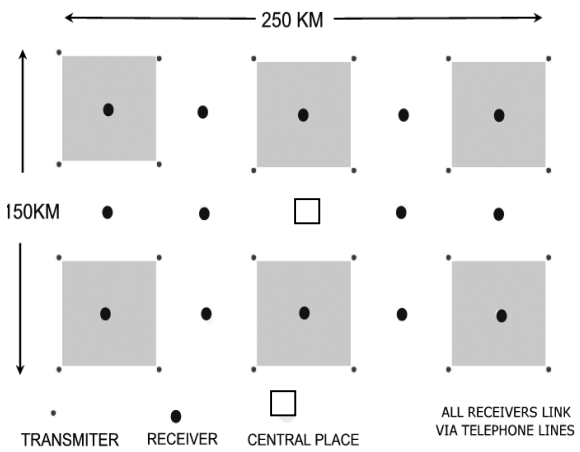

Fig. 14: Grid of UHF/VHF links for monitoring high seismicity region

The sensitivity of any commercially available UHF receiver is typically 0.3 μ Volt @ 12 dB SINAD. Which is equivalent to –146 dB of input power. Input to, four receiver sets operated at different spot frequencies and installed at each black dot point, can be through different fixed attenuator in the range of 10 to 30 dB (assuming received signals strength for all four receivers is maintained equal at around –105 dB). The data of signal strength from all receivers can be digitized at low frequency typically 5-10Hz and sent to the central place on telephone lines. The signals from the entire network can thus be monitored centrally.

On daily basis the RF noise envelop due to stress front would rise by about 10-15 dB, which would result in at least one of the receiver (with maximum input attenuation) generating noisy signal. The rocks under stress would emit higher RF noise just before it reaches the breaking point[8+9] and can provide an alarm for the impending earthquake in the close vicinity. This higher RF noise envelope can be witnessed (on daily basis) for few days before the impending earthquake.

Direct RF noise measurement in the UHF/VHF bands can also be carried out using the multi-channel system adopted[5].

RF emission, an earthquake precursor: probably caused by the planetary alignments:

As illustrated in Fig 7-13, it was observed (during 5th - 11th March) that the RF emission signal strength increased steadily (with increasing stresses) knocking down the different links at different times (based upon received signal strength of different station signals). The RF emission signal strength remained high for few minutes when bulk of the radio links was inoperative. Finally this RF emission signal strength decreased steadily bringing back the links with higher signal strength first, followed by the other links with lower strengths, in decreasing order. The steady increase and then decrease of this RF noise were due to steady increase and decrease in the regional stresses, which could have been attributed by planetary position. Following two paragraphs provides explanation for this phenomenon.

According to a paper[10] on "Planetary configuration: Implication for Earthquake Prediction and Occurrence in South Peninsular India", if two or more than two planets, Sun, Moon are aligned more or less in line (0° or 180°) then the earth would be caught in the middle of a huge gravity struggle between the Sun and the planets. The gravitational stresses would change the speed of the earth in its orbit. When the speed of rotation of earth changes the tectonic plate motion is also affected, just as people collide with each other when the bus driver suddenly applies the breaks. Thus the planetary forces act as a triggering mechanism for the accumulated stress to be released abruptly. The total force of the planets in alignment acts at the epicenter in the direction opposite to the rotation of the earth.

For any earthquake to be triggered at a particular place two condition should satisfy. 1. Triggering distances (TD) and 2. Direction of force acting at the possible epicenter. Considering the total circumference of the earth ~ 40,072 km, the wavelength λ = 20,036 km. = ½ circumference of the earth. The planetary position with regards to earth is measured as Right Ascension (RA) representing Longitude in celestial sphere and Declination (Dec.), representing Latitude in Celestial sphere. The possible epicenter would be at distance of $0.125*\lambda/4$, $0.25*\lambda/4$, …..$1*\lambda/4$ and so on, from the projected planet position of the earth. This distance works out to be 626.125 km or whole multiples of this number[10].

Thus the external force from the planetary alignment, would be acting on many points on the earth simultaneously. If any of these points fall in the seismic zone, which has matured for earthquake and the force is acting in right direction, then <u>this could directly trigger earthquake OR it can make this region vulnerable and earthquake can occur within few days</u>. Due to the rotational motion of the earth, the surface of the earth where the planetary alignment would be acting is a changing phenomenon. For any specific seismically potential place which would be at a triggering distance from a particular position of planetary alignment (on earth), the huge gravitational effect would be seen once in a 24 hours when earth position itself at the same spot once in every 24 hours. The speed of the rotation at earth at equator is around 1670 km/h, which works out to be around 27.82 km/min. As the earth revolves at this speed uniformly, the planetary alignment approached the key position (on earth), from where the Valsad earthquake area was at a triggering distance. Due to the steady speed of rotation, it resulted in linear transformation from no

stress to high stress at the earthquake area. This was represented by the steady rise of the RF noise envelope. Again when the planetary position displaced from that key position again due to earth rotation, linear transformation takes place in the reverse order and RF noise level falls steadily. The phenomena repeats for seven consecutive days due to the planetary alignment of Mercury & Sun, which remains almost unaltered.

Considering the planetary position on 4th and 5th March at 00.00 hours, it is seen that RA and Declination of Sun and Mercury were equal which means both these planets were in conjunction (in line with earth on same side of earth), Jupiter (Ra = 8H28M, Dec = +19º 53.3') and Saturn (Ra = 20H20M, Dec = -19º 44.6') were in opposition (in line with earth but on opposite sides). One of this planet positions (mostly by Mercury-Sun-earth alignment) probably produced some kind of gravitational waves, which developed considerable pressure at the at the earthquake site (Valsad), which was probably at the triggering distance (TD) and also the direction of force was acting in right direction at the earthquake site.

Second case is Chilean earthquake of 22nd May 1960 (Mb = 9.5). This is the biggest event recorded in the history so far. Dr Warwick and others of Radio-physics Inc. Boulder, Colorado, in their paper[11] have provided the details of network of worldwide radio receivers for cosmic radio noise at 18 MHz. Apart from these, the Boulder radio observatory operated a radio interferometer operated at the same frequency, (18 MHz). Six days prior to this Chilean earthquake, on May 16, 1960 between 0350 – 0410 GMT, these stations, which were part of sudden cosmic noise absorption (SCNA) network, received unique RF signal, simultaneously. Dr Warwick and others termed this as signal, which did not come from any outer space and came within earth possibly from the region of this great earthquake. This signal traveled through multiple reflections between ionosphere and earth surface and reached different destination sprawled thousands of km. As per this paper, this is a single incident and the phenomena were not repeated at any other time.

Considering the planetary position at the time of this impact, the Sun and Mercury were in conjunction (with earth). However huge gravitational impact was possibly created by the Moon, which came in opposition with Uranus (with respect to earth] at this time (RA diff. of 1 hour (15 degrees), Dec difference of 1 degree approx.). Just about 24 hours prior to this, Moon was in conjunction (with respect to earth] with Saturn (RA diff of 1 hour (15 degrees), Dec. difference of 4 degree approx.) and most probably both these alignment must have caused huge gravitational forces and would have resulted in emission of broadband RF signal from this earthquake prone area. Since the Moon is the closest celestial body, within the next rotation of the earth, it had moved considerably away from alignment position and the phenomena of RF emission did not repeat on subsequent days as was observed in case of Valsad RF emission from 5th to 11th March 1991.

Earthquake/Volcano Precursor- Date -Time	Lat –Long Quake/volcano place	Planet aligned	Right Ascension	Declination	Effective Longitude [Earth position]	Triggering Distance [TD]
Valsad: 05.03.1991 Time = 00.00 GMT	20.37^0 N-73.18^0 E	Sun-Mercury	22H56M	-6^0, 43.1'	4H 26 M [66.5^0 E]	**3105.52 km**
Chile 16.05.1960 Time = 0400 GMT	39.50^0 S-74.50' W	Sun-Mercury	3H27M	$+18^0$ 48.2'	-8.25^0 W	9850.75km
Chile 16.05.1960 Time = 0400 GMT	39.50^0 S-74.50' W	Moon-Uranus	20H 20M	-15^0 36.8'	-119.66^0 W	**5685 km**
Mt Mihara Volcano 03.11.86 0000 GMT	34.75^0 N-139.225^0E	Venus - Moon	14H 40M	-20^0 23.4'	5h 12 M [75.2 E]	**9405 km**
Mt Mihara Volcano 04.11.86 0000 GMT	34.75^0 N-139.225^0E	Mercury - Moon	15H44M	-22^0 23.2'	6H 16M [90.266E]	8375.3 km

Table 3: Planetary Configuration for two earthquake sequences and one volcano eruption. Timings of the first EM emission precursors are provided. Two sets of planetary alignments were considered for Chile earthquake and Mt Mihara volcano eruption and triggering distance provided in bold letters provide near whole multiple of 626.125 km = 0.125 of λ/4 (wavelength λ = 20,036 km = 0.5 circumference of the earth).

The third case is Volcanic eruption at Mt Mihara in Japan. RA of Venus and Moon matches on 2nd Oct at 1200 hours, where as the declination for both these planets matches exactly at 0000 hours on 3rd Oct. At this time the semi diurnal RF emission had commenced. Just after 12 hours later Moon-Mercury came in conjunction with the earth and the combined effect of all these alignment must have initiated a huge gravitational force. Mt Mihara is located close to Ohshima Island (34.75º N, 139.25º E approx.).

Table 3 provides the details of planetary position, triggering distance etc. in all above cases.

Discussion:

1. EM emission related to earthquake and Volcano: It is believed that the RF emissions come directly from the crystalline rocks of the crust. These rocks provide some sort of a piezoelectric effect when subjected to stress. In a semidiurnal type of RF emission, the timings of the stresses developed were seen consistently twice during the day which were centered on the mid day (local time). G P Tamrazyan[12] provides one of the most probable reasons for this phenomenon. Earth is subjected to ± acceleration in sinusoidal waveform of 24 hours period and with peak values of around 110m/sec^2. He has suggested that the earthquakes frequencies increase during the increasing negative acceleration of the earth as it revolves around itself. This period of negative acceleration corresponds to local timings from 0600-1800 hours approximately. He has also provided energy release diagrams of the earthquakes for three major regions of the earth on 24 hours basis. Two major timings during the day, provides large energy release for maximum negative angular acceleration. This supports predominant RF emission twice during the day due to stresses developed (as illustrated in table 1). There could be some temporal and spatial variation of these timings, which are mostly centered on the mid day.

The EM emission of semidiurnal type is associated on the earth surface due to stresses, which could be contributed by the Sun position. Similar type of EM emissions on the moon surface could be caused by Sun-earth system. As seen in all these examples the timings of these emissions are at time intervals equally spaced from the local noontime. This is a daily phenomena and the rise in the intensity of the EM emission, is attributed by the region, which is matured for earthquakes. Earthquakes/Volcanic eruptions were consistently found during the timings of these EM emissions, which are the result of stresses developed during these timings. The six examples provided, proves such emission was observed in a broad frequency band from VLF to Microwave range.

During the application of semi-diurnal stresses, which results in RF emission, does not seem to be localizing phenomena. The entire rock in the vertical column (few km wide) could contribute to emission under stress. However the region close to seismic fault when matured can provide higher emission prior to an impending earthquake.

The type of emission observed at Bhatsa and also observed at other places (with regards to Chilean earthquakes and eruption of Mt Mihara Volcano) does provide correlation with the rotation of the earth. However, this semi-diurnal RF emission observed on daily basis does not provide any correlation with the lunar tidal forces, which is considered as another triggering source for earthquakes[13].

The EM emission in UHF band was witnessed for about two months even after the Valsad earthquake sequence. This is possible when most stored energy is released during the occurrence of earthquakes, the region may provide EM emission at lower level when not enough energy was left in the area to be released in the form of earthquakes. This is seen in many other examples[14].

2: Monitoring EM Emission related to earthquake and volcanoes: A method of utilizing grid of RF network in the high seismicity area and monitoring RF emission in HF-VHF-UHF band should provide good clues of any impending event. Unlike other methods here one can monitor the emission on daily basis, which is predominantly seen twice around local noon timing and any increase in this emission can be monitored precisely. The utilization of VHF and HF band could broaden the technique for use in the detection of precursors for normal and deep focus earthquakes. The technique effectively can be used for monitoring large size area.

3. Study of temporal and spatial variation of the time-offsets: In the six examples shown in table 1, the timings of semidiurnal emission provide different time-offset (displacement) from the local noontime from ± 1.5 hours to ± 5 hours. At Bhatsa seismic telenet it was experienced that this time-offset is not fixed. Although it does not vary on day-to-day basis but indicate different timings for different periods. During the Valsad earthquake sequence of April 1991, it was found to be ± 4 hours while in the helical record of July 1993, this time –offset was found to be ± - 6 hours.

Continuous data synodic phase versus occurrence time of RF emission for station 12 and 16, in which the maximum amplitude associated with RF spikes, exhibit a sinusoidal behavior consistent with the varying length of the lunar synodic month. Similar behavior is also witnessed in the timings of temporal variation of monthly average values of “tm” and “te” for phase and amplitude of VLF signal which shows

good correlation with the varying day period from Oct to April at Inubu, Japan[6].

The other four cases are different than the above two examples and in general the temporal and spatial variation in these time-offsets with respect to the local noontime need to be studied systematically, which shall provide some clues about the cause of such timely stresses being built within the body of the earth.

4. Possible event sequence, which results in an earthquake: Two cases of RF emissions of diurnal type from Valsad earthquake sequence (initial portion) and emission at 18 MHz in related to Chilean quake were discussed earlier. Both these cases are very rare since they have recorded RF emissions presumably due to the gravitational force of the planetary alignments. Similarly, in case of Mt. Mihara volcanic eruption sequence, the semidiurnal RF emission pattern seems to have initiated by the planetary alignment although there is no recorded RF emission observed.

As per Dr. Venkatnathan[10], most earthquakes occur within +/- 1-3 days of formation of planetary alignment the planetary forces acting as a triggering mechanism for the accumulated stress to be released abruptly. The total force of the planets in alignment acts at the epicenter (if it falls within the triggering distance) in the direction opposite to the rotation of the earth. In few instances the occurrence of the earthquake is not instantaneous and these planetary forces would make this earthquake prone area more vulnerable. As seen in above examples, during the application of semi diurnal stresses acting on daily basis, the region provides higher emission of the RF noise. The phenomenon continues for a few days and subsequently results in the occurrence of earthquake during the application of one such semidiurnal stress.

The sequence of events seen in all these cases can be as follows:

A. Initially each one of these areas would be under stresses due to perpetual motion of the tectonic plates.
B. Earthquake sequence OR volcano eruption sequence initiated with the gravitational force from the planet alignment acting on the specific point on the earth which would be at the triggering distances from this areas in respective cases. Earthquake occurs within ± 1-3 days in majority of the other cases, however in these cases the place becomes very vulnerable.
C. In some other cases, the area could become vulnerable even naturally without the planetary forces acting on it. The vulnerable area is then subjected to the semidiurnal stresses during the daytime at the timings equally spaced [in time domain] from the local noontime. This stage lasts for few days.
D. Finally the vulnerable area gives up during the timings of semidiurnal stresses, resulting in an earthquake/ volcanic eruption.

Figure 15 illustrates the block diagram of possible event sequence, which results in an earthquake.

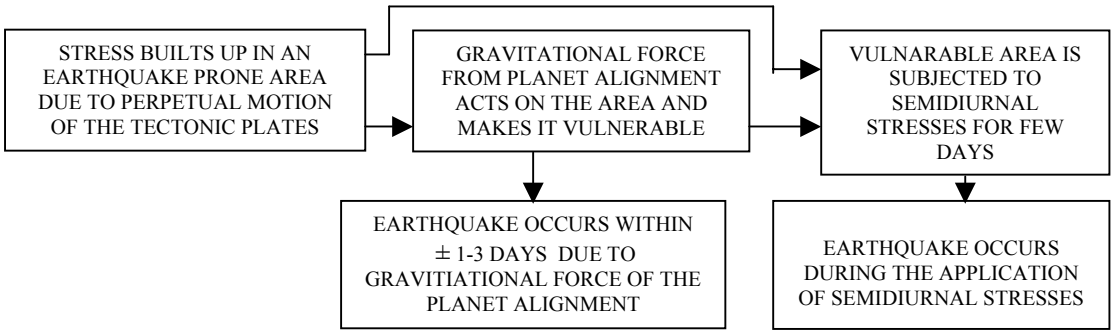

Fig. 15. Block diagram illustrates the possible event sequence, which results in an earthquake.

Acknowledgements: I am grateful to Dr. R S Chaughule, Dr. S L Wadekar Dr. M Ramanmoorthy for various discussions about the manuscript of this write up.

References:

1. Kolvankar V G, Nadre V N , Arora S K and Rao D S, Development and deployment of radio telemetered seismic network at Bhatsa, Current Science's special issue on Seismology in India - an overview. Vol. 62 Nos. 1 and 2, 25th Jan 1992.

2. Gokhberg M B, Morgounov V A and Pokhotelov, EARTHQUAKE PREDICTION SEISMO ELECTROMAGNETIC PHENOENA (pages 112-113), Institute of Earth Physics, Russian Academy of Science Moscow, Russia. Gorden and Breach Publication.

3. Yamamoto Isao, Kuga Kiyoshi, Okabayashi Tohru and Takashi Azakami, System for earthquake prediction research in the region of VHF frequency band, Journal of Atmospheric Electricity, Vol. 22, No3 pp 267-275,2002

4. Haykawa M, Molchanov O A, Tondoh T and Kawai E, The precursory Signature effect of the Kobe earthquake of VLF sub-ionospheric signals, Journal of the Communication research laboratory, Vol. 43 No. 2 July 1996 pp 169-180.
5. Bulow R C, Johnson C L, & Shearer, New events discovered in the Apollo Lunar Seismic Data, Journal of Geophysical Research Vol. 110, E10003, doi:10.1029/2005, 5JE002414,2005.
6. Yoshino Takeo and Tomizawa Ichro (1989), Observation of low frequency electromagnetic emissions at precursors to the volcanic eruptions at Mt. Mihara during November 1986, Physics of the earth and Planetary Interiors, V 57 Issue 1-2, p. 32-39.
7. Kolvankar V G, Earthquake Sequence of 1991 from Valsad Region, Guajrat, BARC-2001/E/006.
8. Ogawa T, Oike K, and Miura T, Electromagnetic radiation from rocks, J. Geophysics Res., 90, 6245-6249,1985.
9. Yamada I, Masuda K and Mizutani H, Electromagnetic and acoustic emission associated with rock fracture, Physics of the earth and Planetory interiors, 57 [1989], 157-168.
10. Venkatanathan N, Rajeshwara Rao N, Sharma K K and Periakali P, Planetary Configuration: Implication for earthquake prediction and Occurrences in South Peninsular India, J. Ind. Geophysics. Union [Oct. 22005], Vol. 9, No4, pp 263-176.
11. Warwick J W, Stoker C and Meyer T R, Radio emission associated with rock fracture: Possible application to the Great Chilean earthquake of May 22, 1960J. Geophysics Res. 87, 2851-2859, April 1982.
12. Tamrazyan G P, Principal regularities in distribution of major earthquakes relative to solar and lunar tides and other cosmic forces, ICARUS 9, 574-592,1968.
13. Sachiko Tanaka, Masakazu Ohtake and Haruo Sato, Evidences for tidal triggering off earthquakes as revealed from statistical analysis of global data. J. Geophysical Research Vol. 107 No. B10, 2211 doi:10. 1029/2001 JB001577, 2002
14. Hata M, Takumi I,Yahashi S and Yasukawa H, Electronic Wave radiation due to the possible plate slip at the central shizuoka Earthquake and to the Island Diastrophism and Volcanic Eruption in Miyake Island, www.ursi.org/Proceedings/ProcGA02/papers/p0661.pdf